

## Vapor Growth Carbon Fiber Felt as an Efficient Interlayer for Trapping Polysulfide in Lithium-Sulfur Battery

Jianna Deng<sup>1</sup>, Jing Li<sup>1,\*</sup>, Jianqiang Guo<sup>2</sup>, Min Zeng<sup>1</sup>, Dan Zhao<sup>3</sup>, Xia Yang<sup>1</sup>

<sup>1</sup> School of Materials Science and Engineering, Southwest University of Science and Technology, Mianyang 621010, China

<sup>2</sup> College of Chemistry, Chemical Engineering and Materials Science, Soochow University, Suzhou, 215123, China

<sup>3</sup> Sichuan Xi'ke Six Timbers Hi-tech Corporation, Mianyang 621010, China

\*E-mail: [195216521@qq.com](mailto:195216521@qq.com)

Received: 29 October 2017 / Accepted: 11 December 2017 / Published: 6 March 2018

Lithium-sulfur (Li-S) batteries with high theoretical specific capacity and energy density are considered as one of the most promising electrical energy storage applications. However, the practical use of Li-S batteries is hindered mainly due to the serious polysulfide shuttling phenomenon. Therefore, the best way to enhance the electrochemical performance of Li-S battery is controlling the shuttling effect caused by the dissolution of polysulfide in the electrolyte. Herein, three different carbon felts were prepared by using vapor growth carbon fiber (VGCF), activated carbon (AC) and super P (SP), respectively, and were used as interlayer between cathode and separator to trap intermediate polysulfides. As a result, the Li-S battery with VGCF interlayer showed high specific initial discharge capacity of 1262 mAh g<sup>-1</sup> and superior cycling performance (836 mAh g<sup>-1</sup> after 100 cycle) at 0.1C.

**Keywords:** lithium-sulfur battery, carbon interlayer, polysulfide, electrochemical performance

### 1. INTRODUCTION

Entering a new era of green energy, many issues including the cost, cycle life, safety, efficiency, energy and electricity need to be taken into account in the development of transport and power storage systems [1-2]. Among existing energy storage systems, lithium-sulfur (Li-S) batteries, using abundant and environment friendly elemental sulfur as the cathode material and metal lithium as anode, have become one of the most promising candidates for next-generation energy storage devices because of their high theoretical energy density and low cost [3-4]. The practical application of Li-S battery with high theoretical specific capacity of 1675 mAh g<sup>-1</sup> based on the chemical conversion reaction of  $S_8 + 16 Li^+ + 16 e^- \rightarrow 8 Li_2S$  is impeded by the notorious shuttling phenomenon and low

conductivity of sulfur. Many measures have been taken to solve those problems, which include porous host materials for sulfur impregnation [5], interconnected conductive networks[6], conductive interlayers [7], solid and gel electrolytes [8] and 3D lithium hosts [9]. In past years, a large number of literature are related to carbon materials used in the cathode to improve the performance of lithium-sulfur battery. Recently, some studies on the application of interlayers in the Li-S batteries are reported. For example, the graphitic carbon fiber felt [10], MWCNT [11], carbonized cellulose paper [12], carbon fiber cloth [13] were used as interlayer to analyze the electrochemical property of interlayers in lithium-sulfur batteries. Su et al [14] made a microporous carbon paper as a bifunctional interlayer shows great cycle stability and rate performance, which the first discharge capacity was as high as 1367 mAh g<sup>-1</sup> and the capacity maintained above 846 mAh g<sup>-1</sup> for 70 cycles when it was cycled up to 3C.

In this work, we report the application of vapor growth carbon fiber which form a favorable electronic transmission channel, reducing the electron transport path and the charge transfer resistance, as a cheap and effective interlayer for Li-S batteries. In order to demonstrate the effectiveness of such simple interlayer and highlight the excellent performance of VGCF, sulfur was directly used as the cathode in this study. The final results show that the electrochemical performance of the VGCF interlayer is better than that without interlayer, consistent with our expected results.

## 2. EXPERIMENTAL

### 2.1. Material preparation

The PTFE emulsion (Aladdin, AR) was mixed with VGCF (Shenzhen, AR), SP (Shenzhen, AR) and AC (Shenzhen, AR) at a mass ratio of 3: 2, respectively. Then, the mixture was added into ethanol to form solution. After that, the solution was condensed into a plasticene-liked solid under magnetic stirring for 12 hours. The plasticene-liked solid was pressed into a film (thickness: 150µm) by a twin roller, dried at 70°C in a vacuum, and finally punched into a carbon interlayer with a diameter of 15 mm.

### 2.2. Materials Characterization

The morphology and crystal structure of the carbon material and interlayer were identified by scanning electron microscopy coupled with the EDX and elemental map results(SEM, Ultra55).

### 2.3. Cell Assembly and Electrochemical measurement

The cathode slurry was prepared by mixing sulfur (70%), conductive carbonblack(20%) and polyvinylidene uoride (PVDF 10 wt%) binder in N-methyl pyrrolidinone (NMP) solvent. The slurry was then coated onto aluminum foil to make cathode electrode. Before assembling cell, sulfur cathode and carbon interlayer are dried at 70°C in a vacuum for 24h. CR2016 coin-type cells was assembled

with metallic lithium foil and separator (Celgard 2400) in glovebox filled with argon. Bis-(trifluoromethanesulfonyl)imide (LiTFSI, 1.0 M) with  $\text{LiNO}_3$  (0.2M) dissolved in 1,3-dioxolane (DOL, J&K) and 1,2-dimethoxyethane (DME, J&K) (v/v, 1:1) was used as electrolyte. The schematic of carbon interlayer of Lithium-sulfur battery was shown in (Fig.1).

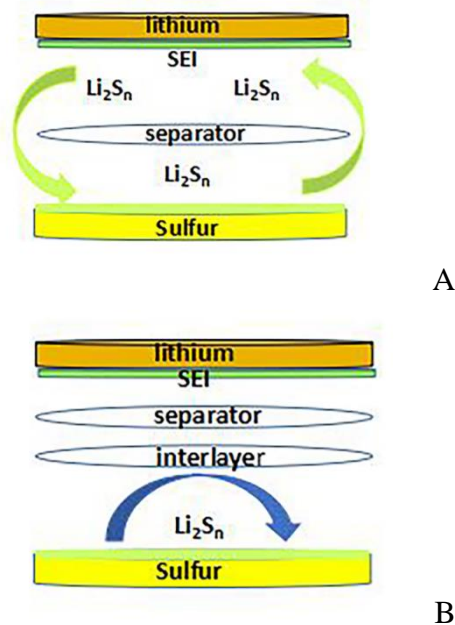


**Figure 1.** Comparison of effect on trapping polysulfide in lithium-sulfur battery (a) without and (b) with carbon interlayer.

The galvanostatic charged/discharged tests were performed at different rates in the voltage range of 1.5-3.0V on LANDCT2001A battery tester. Cyclic voltammetry measurements were carried out with a scan rate of  $0.1 \text{ mVs}^{-1}$  between 1.5 and 3.0 V on an electrochemistry workstation (CHI660E). Electrochemical impedance spectra (EIS) were measured by electrochemical workstation (CHI660E) with a disturbance amplitude of 5 mV in the frequency range of 0.1 Hz to 100 kHz.

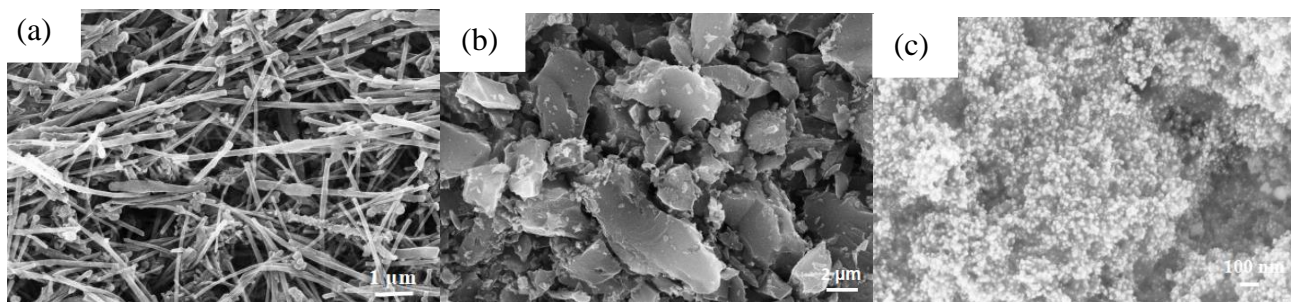
### 3. RESULTS AND DISCUSSION

#### 3.1. Structure and morphology analyses

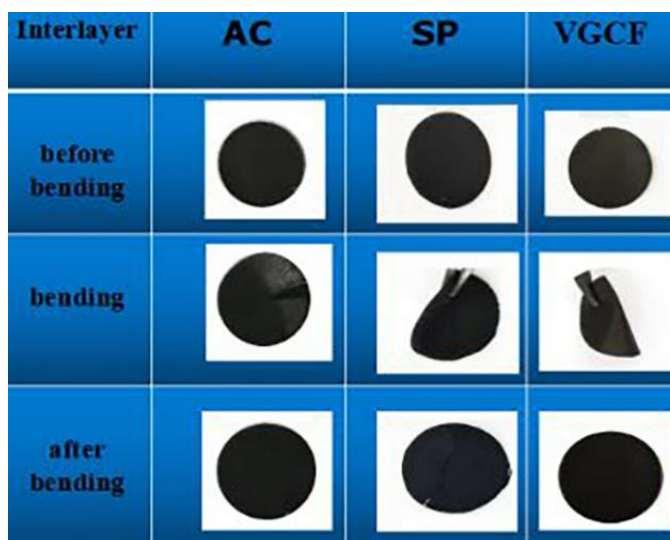
Fig. 2 shows the SEM images of VGCF, AC and SP. The morphologies of three carbon materials can be observed clearly. Super P consist of spherical particles (Fig.2c) and the shape of AC is irregular and angular, whose surface are filled with pore structure (Fig.2b). As the Fig.2a shows, the morphology of VGCF is a cross-conductive fiber, which form a favorable electronic transmission channel, reducing the electron transport path and the charge transfer resistance.

In order to verify the strength and flexibility of the different carbon interlayers, a simple bending experiment was carried out. As shown in Fig. 3, AC and SP interlayer had produced cracks

after bending, however, the VGCF interlayer presents a good mechanical strength and flexibility, so that Li-S cell can keep a robust stability during its assembly and cycling.

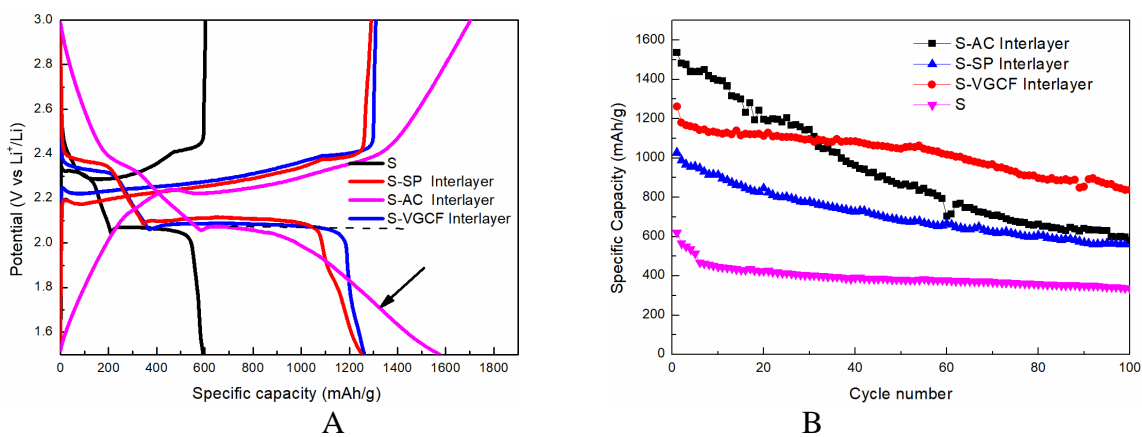


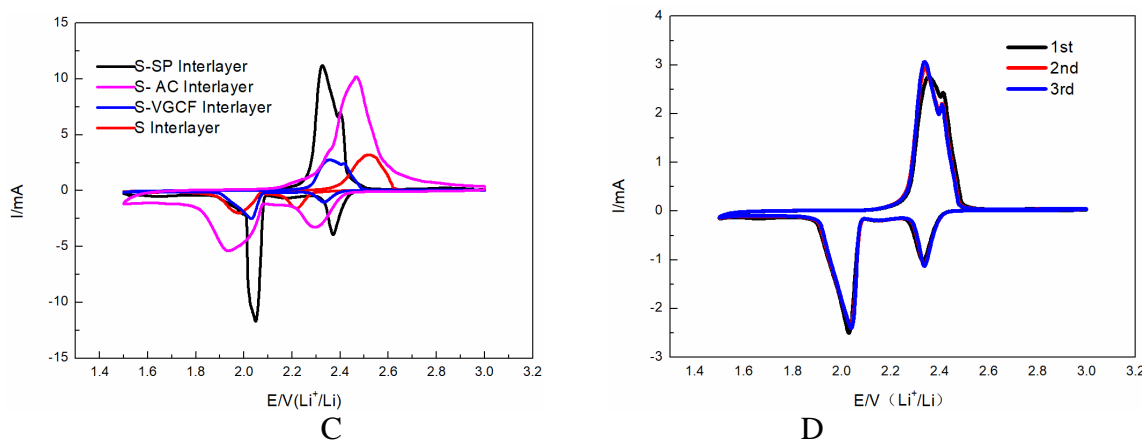
**Figure 2.** SEM of three different carbon materials (a) VGCF, (b) AC and (c) SP.



**Figure 3.** The exhibition of strength and flexibility of three different carbon interlayer.

### 3.2. Electrochemical performance of Li-S battery using carbon interlayer





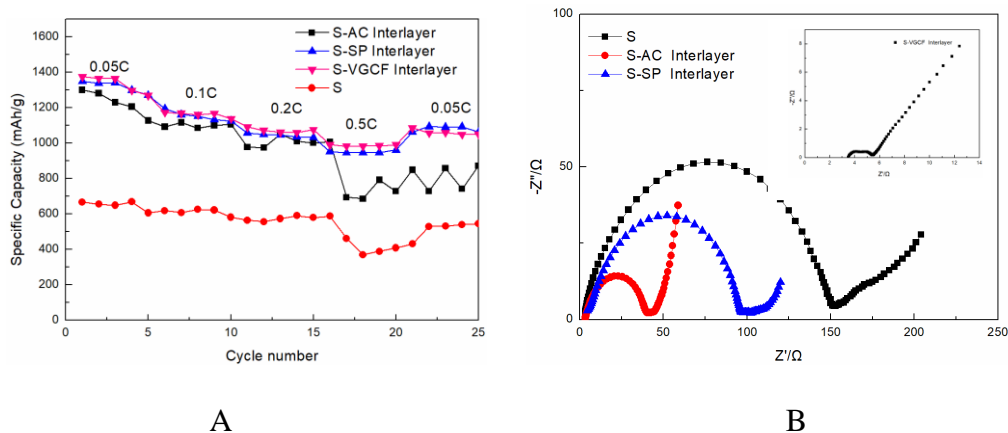
**Figure 4.** (a) Initial discharge-charge profiles; (b) the cycle performances; (c) cyclic voltammogram profiles of Li-S battery with and without carbon interlayer at scanning rate of  $0.1\text{mV s}^{-1}$ ; (d) cyclic voltammogram profiles of Li-S battery with VGCF interlayer in the first 3 cycle.

Fig.4a shows the galvanostatic charge/discharge profiles of Li-S battery with and without carbon interlayer. The curves look similar: two discharge plateau are observed at around 2.3 and 2.1 V, which are related to the transformation of sulfur to soluble lithium polysulfide ( $\text{Li}_2\text{S}_n$ ,  $4 \leq n \leq 8$ ) and reduction of long-chain soluble lithium polysulfide to insoluble  $\text{Li}_2\text{S}_2$  and  $\text{Li}_2\text{S}$ , respectively [15-18]. After calculation, the initial discharge capacity of Li-S battery using VGCF and SP interlayer are  $1262\text{mAh g}^{-1}$  and  $1027\text{mAh g}^{-1}$  at the rate of  $0.1\text{C}$ , respectively. The first discharge capacity of Li-S battery with AC interlayer is  $1536\text{mAh g}^{-1}$ , which is the highest capacity value among three carbon interlayers. This is attributed to the extra capacity contribution of AC as supercapacitor material, which can be confirmed by the shape of charge/discharge profiles between 1.5-2.0 V (marked with black arrow). However, in terms of the cycling performance, the optimal candidate belongs to Li-S battery with VGCF interlayer rather than AC interlayer. As shown in Fig.4 b, the specific capacity for AC interlayer Li-S battery declines to  $580\text{mAh g}^{-1}$ , whereas the capacity of VGCF interlayer remains as high as  $836\text{mAh g}^{-1}$  after 100 cycle. The excellent electrochemical performance of VGCF interlayer Li-S battery is ascribed to its unique morphology, which forms a favorable electronic transmission channel and reduces the electron transport path and the charge transfer resistance[19-20]. To further explain the obtained observations in our experiments, cyclic voltammetry at scanning rate of  $0.1\text{mV s}^{-1}$  were carried out (Fig.4c). The profiles look similar: two reduction peaks and one main oxidation peak, which is consistent with the previous reports. Two reduction peaks are observed around 2.3 and 2.0 V, which are related to the reduction of sulfur to soluble higher-order lithium polysulfide ( $\text{Li}_2\text{S}_n$ ,  $4 \leq n \leq 8$ ) and reduction of soluble lithium polysulfide to insoluble  $\text{Li}_2\text{S}_2$  and  $\text{Li}_2\text{S}$ [21-22], respectively. In order to deeply investigate the capacity contribution of VGCF interlayer, we perform CV of VGCF interlayer of first 3 cycle in Fig.4 d which show both the polarization phenomenon and resistance are relatively small, which reduce the charge transmission resistance and is conducive to the battery capacity.

Fig.5a shows the discharge capacity comparison of Li-S battery without interlayer and with AC interlayer, SP interlayer and VGCF interlayer at various rates. As shown in Fig. 5(a), cells with VGCF interlayer exhibited stabilized discharge capacities of  $1376$ ,  $1270$ ,  $1092$  and  $992\text{mAh g}^{-1}$  at

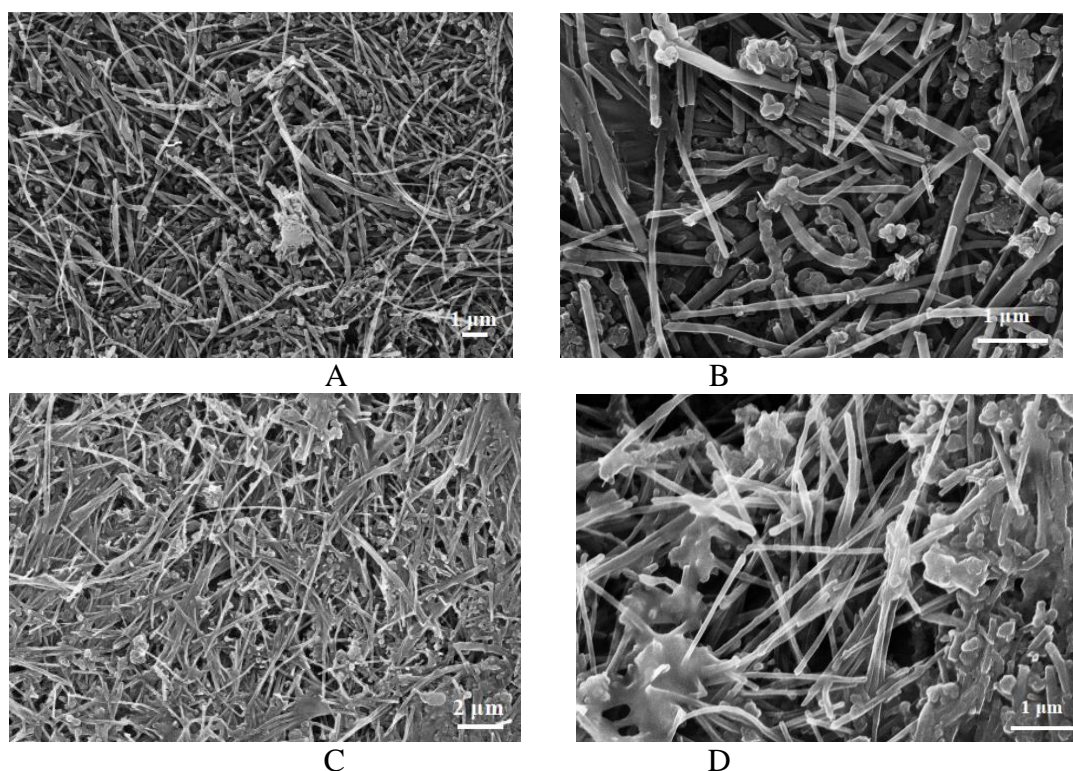


0.05, 0.1, 0.2 and 0.5 C rates, respectively, while for cells with AC interlayer, SP interlayer and without interlayer, the corresponding capacities were lower than that of VGCF interlayer. These results clearly manifest the outstanding rate capability of Li-S cell with VGCF interlayer under various current densities conditions.



**Figure 5.** (a) Discharge capacity comparison of Sulfur electrodes without interlayer and with AC interlayer, SP interlayer and VGCF interlayer at various rates. (b) EIS spectra of sulfur electrodes and with AC interlayer, SP interlayer and VGCF interlayer.

Electrochemical impedance spectroscopy (EIS) is a available tool to investigate the internal resistance of Li-S batteries [23]. The diameter of the semicircular portions of the curves in Fig. 5b represents the charge transfer resistance( $R_{ct}$ ), which is mainly produced at the interface between the electrode and the electrolyte [24-25].



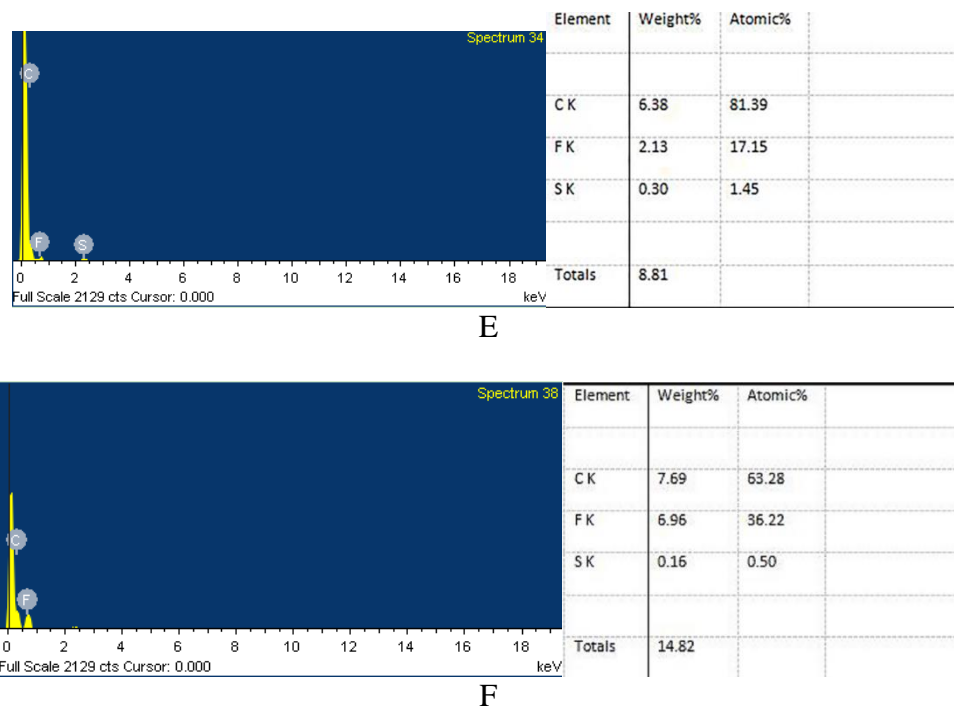


**Figure 6.** SEM and the corresponding magnification of VGCF interlayer before (a、 b) and after (c、 d) 100 cycle, EDX of two side of VGCF interlayer (e) the side near the cathode, (f) the side near the separator.

As shown in Fig. 5b, the charge transfer resistance ( $R_{ct}$ ) of VGCF interlayer is much smaller than that of sulfur electrodes without interlayer and with AC interlayer and SP interlayer, indicating improved electron conductivity due to its cross-conductive network.

The scanning electron microscopy of the VGCF interlayer before and after cycles and the corresponding EDX were used to demonstrate the absorption of polysulfide by the conductive interlayer. As shown in Fig.6 a, VGCF are evenly distributed in the PTFE, the corresponding magnification can be seen clearly in Fig.6b shows that the morphology of VGCF after preparing into carbon interlayer is very complete. The SEM of VGCF interlayer after 100cycle present in Fig.6 c and Fig.6 d, it can be seen that the morphology of VGCF are as complete as before the cycle, and no corrosion deformation occurs. At the same time, it can be seen that the VGCF surface adsorbs some polysulfides. In order to demonstrate the absorption of polysulfide in the VGCF interlayer, we performed the EDX test on both sides of the interlayer. The results are shown in Fig.6 e and Fig.6 f. The sulfur element was detects according to the results of the EDX of the VGCF interlayer near cathode side , but there was rare sulfur content near the separator side. The results clearly demonstrate that the VGCF interlayer has a significant adsorption effect on polysulfide, and the polysulfide is adsorbed in the VGCF conductive network structure.

#### 4. CONCLUSIONS

In this paper, three kinds of carbon interlayers were prepared by SP, AC and VGCF, and the effects of carbon interlayers on the cycling stability and capacity of lithium-sulfur batteries were

analyzed. The first discharge capacity of VGCF interlayer was 1262 mAh g<sup>-1</sup> at 0.1 C, the capacity remained 836 mAh g<sup>-1</sup> after 100 cycles with the capacity retention rate of above 66%. It confirms that the employment of VGCF interlayer can not only improve the conductivity of elemental sulfur, but also capture polysulfide to prevent the occurrence of shuttle effect. Consequently, the VGCF interlayer would be a promising candidate for the Li-S battery with long cycle stability and high rate capability.

#### ACKNOWLEDGEMENTS

The authors appreciate the support of the LongShan academic talent research supporting program of SWUST(No. 17LZX507).

#### References

1. R. P. Fang, S. Y. Zhao, Z. H. Sun, D. W. Wang, H. M. Cheng and L. Feng, *Adv. Mater.*, (2017).
2. C. Huang, J. Xiao, Y. Y. Shao, J. M. Zheng and Bennett, *Nat. Commun.*, 5 (2014) 3015.
3. H. J. Peng, J. Q. Huang, X. B. Cheng and Q. Zhang, *Adv. Energy Mater.*, (2017).
4. L. L. Kong, Z. Zhang, Y. Z. Zhang, S. Liu, G. R. Li and X. P. Gao, *ACS Appl. Mater. Interfaces.*, 8 (2016) 31684–31694.
5. J. Li, J. Q. Guo, L. Zeng and R. F. Peng, *RSC Adv.*, 6 (2016) 26630-26636.
6. Y. S. Su and A. Manthiram, *Chem. Commun.*, 48 (2012) 8817-8819.
7. V. C. Hoang, V. D. Do, I. Nah, C. Lee, W. Cho, I. Oh, *Electrochim. Acta.*, 210 (2016) 1-6.
8. M. Ling, X. Zhu, Y. Jiang, J. Zhu, *Ionics*, 22 (2016) 1-6.
9. X. B. Cheng, H. J. Peng, J. Q. Huang, R. Zhang, C. Z. Zhao and Q. Zhang, *ACS Nano*, 9 (2015) 6373-6382.
10. K. Dong, W. A. Chi, H. J. Jeon, *J. Power Sources*, 360 (2017) 559-568.
11. Z. L. Ma, L. Zhen, K. D. D. Liu, J. Huo and S. Y. Wang, *J. Power Sources*, 325 (2016) 71-78.
12. S. Q. Li, G. F. Ren, M. N. F. Hoque, Z. H. Dong, J. Warzywoda and Z. Y. Fan, *Appl. Surf. Sci.*, 396 (2017) 637-643.
13. Y. X. Yang, W. Sun, J. Zhang, X. Y. Yu, Z. H. Wang and K. Sun, *Electrochim. Acta*, 209 (2016) 691-699.
14. Y. S. Su, A. Manthiram, *Nat. Commun.*, 3 (2012) 1166.
15. J. Li, J. G. Guo, J. N. Deng and Y. J. Huang, *Mater. Lett.*, 189 (2017) 188-191.
16. Z. C. Yang, J. C. Guo, S. K. Das, Y. C. Yu, Z. H. Zhou, H. Abruñab and L. Archer, *J. Mater. Chem. A*, 1 (2012) 1433-1440.
17. C. Wang, X. C. Wang, Y. J. Wang, J. T. Chen, H. H. Zhou and Y. H. Huang, *Nano Energy*, 11 (2015) 678-686.
18. Z. W. Seh, W. Y. Li, J. J. Cha, Y. Yang and Y. Cui, *Nat. Commun.*, 4 (2013) 1331.
19. Z. B. Xiao, Z. Yang, L. Wang, H. J. Nie, M. E. Zhong, Q. Q. Lai, X. J. Xu, Z. J. Zhang and S. M. Huang, *Adv. Mater.*, 27 (2015) 2891-2898.
20. Y. Hou, J. Y. Li, X. F. Gao, Z. H. Wen, C. Yuan, J. H. Chen, *chen. Nanoscal Commun*, 8 (2016) 8228–8235.
21. X. L. Li, Y. L. Cao, W. Qi, L. V. Saraf, J. Xiao, Z. M. Nie, J. Mietek, J. G. Zhang, B. Schwenzer and J. Liu, *J. Mater. Chem. A*, 21 (2011) 16603-16610.
22. R. S. Song, R. P. Fang, L. Wen, Y. Shi, S. G. Wang and Feng Li, *J. Power Sources*, 301 (2016) 179-186.
23. J. Q. Guo, J. Li, Y. J. Huang, M. Zeng and R. F. Peng, *Mater. Lett.*, 181 (2016) 289-291.
24. K. Zhang, F. R. Qin, J. Fang, Q. Li, M. Jia, Y. Q. Lai, Z. A. Zhang and J. Li, *J. Solid State Electrochem.*, 18 (2014) 1025-1029.



25. H. K. Jing, L. L. Kong, S. Liu and X. Q. Gao, *J. Mater. Chem. A*, 3 (2015) 12213-12219.

© 2018 The Authors. Published by ESG ([www.electrochemsci.org](http://www.electrochemsci.org)). This article is an open access article distributed under the terms and conditions of the Creative Commons Attribution license (<http://creativecommons.org/licenses/by/4.0/>).